Hindawi
Advances in Fuzzy Systems
Volume 2019, Article ID 2042874, 10 pages
https://doi.org/10.1155/2019/2042874

Research Article

On Variable-Universe Fuzzy Control for Drive Chain of Front-End Speed Regulated Wind Generator

Hongwei Li,[1] **Kaide Ren**,[1] **Haiying Dong**,[1,2] **and Shuaibing Li**[2]

[1]*School of Automation and Electrical Engineering, Lanzhou Jiaotong University, Lanzhou 730070, China*
[2]*School of New Energy and Power Engineering, Lanzhou Jiaotong University, Lanzhou 730070, China*

Correspondence should be addressed to Haiying Dong; hydong@mail.lzjtu.cn

Received 24 January 2019; Accepted 4 March 2019; Published 19 March 2019

Guest Editor: Ali Mostafaeipour

The rapid development of wind generation technology has boosted types of the new topology wind turbines. Among the recently invented new wind turbines, the front-end speed regulated (FSR) wind turbine has attracted a lot of attention. Unlike conventional wind turbine, the speed regulation of the FSR machines is realized by adjusting the guide vane angle of a hydraulic torque converter, which is converterless and much more grid-friendly as the electrically excited synchronous generator (EESG) is also adopted. Therefore, the drive chain control of the wind turbine owns the top priority. To ensure that the FSR wind turbine performs as a general synchronous generator, this paper firstly modeled the drive chain and then proposed to use the variable-universe fuzzy approach for the drive chain control. It helps the wind generator operate in a synchronous speed and outperform other types of wind turbines. The multipopulation genetic algorithm (MPGA) is adopted to intelligently optimize the parameters of the expansion factor of the designed variable-universe fuzzy controller (VUFC). The optimized VUFC is applied to the speed control of the drive chain of the FSR wind turbine, which effectively solves the contradiction between the low precision of the fuzzy controller and the number of rules in the fuzzy control and the control accuracy. Finally, the main shaft speed of the FSR wind turbine can reach a steady-state value around 1500 rpm. The response time of the results derived using VUFC, compared with that derived from a neural network controller, is only less than 0.5 second and there is no overshoot. The case study with the real machine parameter verifies the effectiveness of the proposal and results compared with conventional neural network controller, proving its outperformance.

1. Introduction

The recent progress in wind energy generation has advanced the ever-increasing development of large-scale wind generation. As a complex electromechanical system that converts wind energy into electricity, wind turbines are developing in the way of high power, high efficiency, high reliability, and low cost. As the wind is changeable and unpredictable due to its randomness, current studies mainly focus on how to convert such stochastic energy into power electricity smoothly [1, 2]. For such purpose, different kinds of wind turbines have been developed, including the early machine installed with an induction generator, which operates in a constant-speed constant- frequency (CSCF) mode [3], and the recently developed turbines installed with a direct-drive permanent-magnet synchronous generator (PMSG) or with a doubly fed induction generator (DFIG) [4, 5], which operate in a variable-speed constant- frequency (VSCF) mode.

Compared with the CSCF type wind turbines, the wind turbines functioning in a VSCF model can behave more efficiently since they can operate in a maximum power point tracking (MPPT) mode. Since both of the CSCF units and the VSCF units connect to the grid through a back-to-back converter, power quality becomes an important issue to them, which is more urgent to the VSCF type wind turbines since they still cannot meet some of the grid connection requirements automatically, e.g., the low-voltage ride through (LVRT) capability. From such aspect, the CSCF wind turbines have certain advantages compared with the VSCF units as additional facilities like LVRT module, reactive power compensation devices, and filters are not necessarily required. In order to make use of the advantages of both the VSCF type wind turbines and the CSCF type units, thus letting the wind turbine work in a gird-friendly way like traditional thermal power, hydropower, or nuclear power with fewer harmonics and high power quality, great efforts have been

made [6–13]. Related researches done by scholars include the optimized control of the generator [6, 7], the output power and voltage [8, 9], the drive chain [10], and the VSCF system [11]. Coordinated control of the pitch and torque of the turbine are also investigated since higher efficiency can be acquired [12, 13].

However, the intrinsic drawbacks of traditional VSCF wind turbines are obvious since converters are necessarily required by either the PMSG or the DFIG for integrating into the power grid. For DFIG, its converter power is generally one-third of its ratings, which makes the cost of the machine reduce to a certain extent. But it also makes the generator more sensitive to the fluctuation of the power grid, i.e.; once the voltage of grid-side fluctuates, the DFIG is prone to trip and disconnect from the grid. In terms of PMSG, a full-scale power converter is adopted, which makes it no longer sensitive to the voltage fluctuation of the grid-side. But the total cost of the machine, in comparison, is much higher.

For the sake of minimizing the interferences of harmonics generated by voltage source converters on the power grid to the greatest extent, current source based new converter topology and kinds of filters are proposed [14–17]. In [14], J. Birk et al. propose to use a new topology that consists of six parallel-connected power converters; it reduces the total harmonic distortion in current from 6.3% to 2.3% and increase the reliability of the turbine six times as high as before. Similarly, in [15], a current- source inverter topology for large multimegawatt wind turbines is proposed, which helps to reduce the fifth and seventh harmonic content without filtering actions. Also, for the purpose of harmonic reduction, kinds of filters are adopted in [16, 17] in combination with optimized algorithms.

Although types of control methods are proposed, as mentioned before, drawbacks introduced by the converter in wind turbines are inevitable and costly, and the asynchronization of the stator and rotor speed asynchronous generator is also a deficiency compared with the electrically excited synchronous generator (EESG). The control of such machines is realized through, without exception, a converter, which can be seen as a "Back-End" mode. In front of that, prototypes of "Front-End" controlled wind turbines with EESG are proposed and some of them are even converterless [18–20], as shown in Figure 1. By introducing an electromagnetic coupler-based wind turbine, a new machine was proposed by Tsinghua University and United Power [18] (Figure 1(a)). In [19], a gearboxless wind turbine is designed by ChapDrive, which uses a hydraulic system to replace the gearbox (Figure 1(b)), and an EESG is directly linked with power grid without using a converter. Similarly, a new machine called front-end speed regulated (FSR) wind generator designed by Voith Turbo and Dewind is introduced in [20] (Figure 1(c)).

As the converter is reduced, speed regulation of the EESG in Figure 1(c) is realized through WinDrive. Hence, drive chain control of the wind generator becomes the key to keep the machine operating in a VSCF mode without harmonics imported to the grid. However, to the best of the authors' knowledge, the realization of an efficient control for drive chain of the FSR wind generator is not reported at present. Thus, this paper proposes a variable-universe fuzzy method for drive chain control of the FSR wind generator based on a multipopulation genetic algorithm (MPGA), which keeps the generator speed constant at any time.

The rest of this paper is organized as follows: Section 2 details the drive chain model of FRS wind turbine, and implementation of the proposed method is presented in Section 3, while results and analysis are given in Section 4. Finally, conclusions are drawn.

2. Drive Chain Modeling of the FSR Wind Turbine

2.1. The Principle of FRS Wind Turbine. As shown in Figure 1(c), the FSR wind turbine consists of a wheel, a gearbox, a hydraulic torque converter unit called WinDrive, and a directly grid-connected EESG. Unlike conventional "Back-End" machines, the speed regulation of the FSR wind turbine is realized through the drive chain including the gearbox and the WinDrive, rather than a converter. A detailed structure of the FSR wind turbine is given in Figure 2.

In the beginning, the wind wheel is driven by the wind at a speed of V_w, and the main shaft of the turbine consequently rotates with a speed ω_k. The gearbox then speeds the rotation of the shaft from an input speed ω_{g1} to ω_{g2}. After that, the WinDrive will adjust the output speed ω_{g2} of the gearbox to a constant speed ω_G (approximately 1500 rpm), which is called the synchronous speed of the EESG. The WinDrive, as shown in Figure 2, is composed of a set of planetary gears and a hydraulic torque converter; two of them are integrated as a whole. Speed control of the WinDrive is directly realized by regulating the guide vane angle x of the hydraulic torque converter. Therefore, the EESG can work as the generator in a thermal plant and the output power can be regulated by adjusting guide vane angle with reference to the wind speed.

2.2. Modeling of the Drive Chain. For WinDrive, as it can achieve either continuous adjustment of the speed of the main shaft or regulation of the torque in the drive chain, once there appears a sudden change in wind speed, it can release part of the energy stored to increase the damping of the drive chain to smooth the torque. Therefore, the modeling of the drive chain of FSR wind turbine will consider both the speed transfer and the torque delivery.

(1) Speed Relationship between the Wind Wheel and the Planetary Gears. Considering there are three planetary gear sets from the wheel to the EESG, the second and the third planetary gear set satisfy:

$$\omega_t = (1 + b)\,\omega_j - b\omega_q$$
$$c = -\frac{\omega_T}{\omega_q} \tag{1}$$

where b and c stand for the structure parameters of the second planetary gear set; ω_t, ω_j, and ω_q are the rotation speed of the solar wheel, planetary carrier, and the ring of outer gear, respectively. ω_T is the output speed of torque converter.

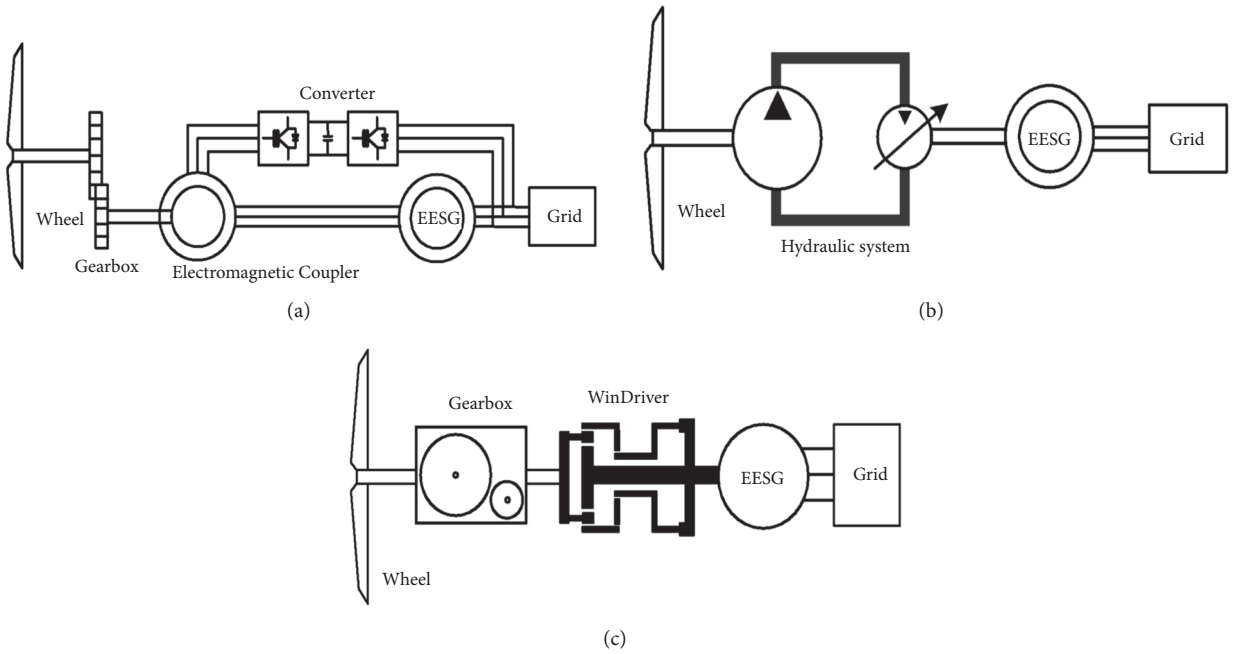

Figure 1: Schematic of front-end speed regulated wind turbines.

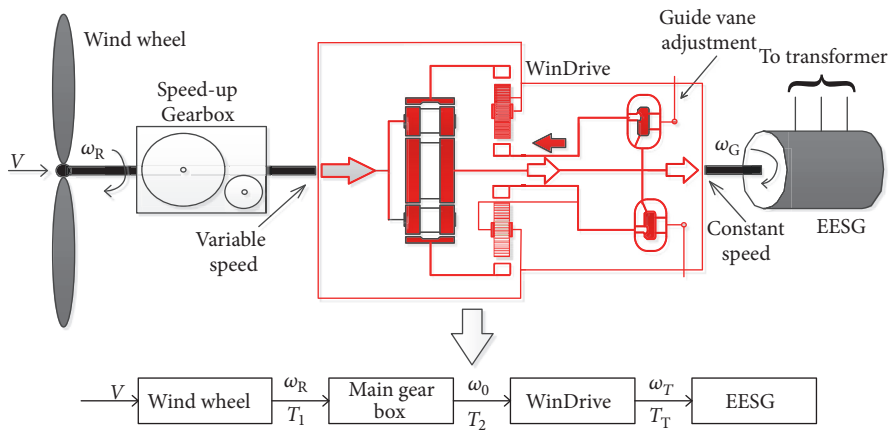

Figure 2: Drive chain of the FSR wind turbine with a hydraulic torque converter (red in the figure).

(2) Aerodynamics Model of the Wind Turbine. Based on Baez's theory, the wind turbines can absorb only a limited amount of energy from natural wind. Actual torque of the wind wheel can be denoted as [21]:

$$T_R = \frac{P_R}{\omega_R} = \frac{1}{2\lambda}\rho\pi R^3 v^2 C_P(\lambda,\beta) \tag{2}$$

with

$$\lambda = \frac{R\omega_R}{v} \tag{3}$$

and

$$C_P(\lambda,\beta) = 0.5176\left(\frac{116}{\lambda_i} - 0.4\beta - 5\right)e^{-21/\lambda_i} + 0.0068\lambda$$
$$\frac{1}{\lambda_i} = \frac{1}{\lambda + 0.08\beta} - \frac{0.035}{\beta^3 + 1} \tag{4}$$

where P_R, T_R, and ω_R represent the mechanical power, the torque, and the rotation speed of wind wheel, respectively. R and β stand for the radius and blade angle of the wind wheel, C_P is power coefficient, and ρ is air density.

(3) Drive Chain Model. From the drive chain structure given in Figure 2, the speed and torque relationship between the

wind wheel and the planetary gear of the WinDrive can be formulated using a rigid axis model:

$$T_R - T_1 = J_R \frac{\mathrm{d}\omega_R}{\mathrm{d}t} + c_1 \omega_R \tag{5}$$

where J_R is inertial of the wheel and T_1 and c_1 are the torque and damping coefficient of the low-speed shaft, respectively.

By neglecting the inertial, the input and output relationship of the gearbox can be described as

$$T_1 = \alpha T_2 \tag{6}$$

where T_2 is the output torque of the gearbox and α is the gear ratio.

The dynamical balance equation of the WinDrive can be formulated as

$$\begin{aligned} T_{t1} - T_B - T_0 &= J_{t1} \frac{\mathrm{d}\omega_0}{\mathrm{d}t} \\ T_T - T_{t2} &= J_{t2} \frac{\mathrm{d}\omega_T}{\mathrm{d}t} \end{aligned} \tag{7}$$

where T_{t1} and T_{t2} are input torque of the solar wheel for the first-grade and the second-grade planetary gear, respectively. T_T is the output torque of the torque converter, T_0 is the input torque of the EESG, J_{t1} is the moment of inertia of the front shaft of the EESG while J_{t2} is the output moment of inertia of the torque converter, and ω_0 is main shaft speed.

Ignoring the moment of inertia of high-speed shaft, its dynamic equation can be summarized as

$$T_0 - T_e = J_e \frac{\mathrm{d}\omega_0}{\mathrm{d}t} + c_e \omega_0 \tag{8}$$

where c_e is the damping coefficient of the high- speed shaft and T_e and J_e are the electromagnetic torque and the moment of inertia of the EESG.

Based on the relationship between rotation speed and torque, the following equation can be obtained from [20, 22]:

$$\begin{aligned} \omega_T &= \frac{c\omega_0 + a(1+b)c\omega_R}{b} \\ \frac{T_{t1}}{1} &= \frac{T_{q1}}{b} = \frac{T_{j1}}{-(1+b)} \\ \frac{T_{t2}}{1} &= \frac{T_{q2}}{c} = \frac{T_{j2}}{-(1+c)} \end{aligned} \tag{9}$$

where T_q and T_j represent the torque of external gear and planet carrier with i indicating the first or the second gear set, respectively. Constant a is the structure parameter of the first planetary gear set.

In the ring of outer gear, the torque delivered by two rings are equivalent, namely, $T_{q1} = T_{q2}$. Besides, when conducting a derivation of the first equation in (9), one can get the following.

$$\begin{aligned} \frac{\mathrm{d}\omega_T}{\mathrm{d}t} &= \frac{c}{b}\frac{\mathrm{d}\omega_0}{\mathrm{d}t} + \frac{a(1+b)c}{b}\frac{\mathrm{d}\omega_R}{\mathrm{d}t} \\ \frac{T_{t1}}{T_{t2}} &= \frac{c}{b} \end{aligned} \tag{10}$$

From the above relationships, the following equation can be obtained:

$$\begin{aligned} J_1 \frac{d\omega_R}{dt} + J_2 \frac{d\omega_0}{dt} + c_1 \omega_R &= f_1 \\ J_3 \frac{d\omega_R}{dt} + J_4 \frac{d\omega_0}{dt} + c_e \omega_0 &= f_2 \end{aligned} \tag{11}$$

with $J_1 \sim J_4$ and $f_1 \sim f_2$ satisfying

$$\begin{aligned} J_1 &= J_R + J_3 \\ J_2 &= \frac{c}{b} J_{t2} \\ J_3 &= \frac{a(1+b)c}{b} J_{t2} \\ J_4 &= J_{t1} + J_e + J_2 \\ f_1 &= T_R + \frac{a(1+b)c}{b} T_T \\ f_2 &= \frac{c}{b} T_T - T_B - T_e. \end{aligned} \tag{12}$$

(4) Torque Converter Model. Based on the results from the previous study [23], the torque of the converter can be formulated as

$$\begin{aligned} T_B &= \rho_{oil} g \lambda_B (i_{TB}, x) n_B^2 D^5 \\ T_T &= a_0 + a_1 i_{TB} + a_2 i_{TB}^2 \end{aligned} \tag{13}$$

with

$$\begin{aligned} \lambda_B (i_{TB}, x) = &\left(-0.2128 i_{TB}^2 + 0.15887 i_{TB} + 1.1815\right) \\ &\times 10^{-6} \end{aligned} \tag{14}$$

where x and i_{TB} are the guide vane angle and the speed ratio of the torque converter, respectively. ρ_{oil} is the density of oil filled in torque converter, which equals 826kg/m^3 in this paper. λ_B and n_B stand for the torque coefficient and speed of the torque converter pump, while D is the diameter of the circular circle, which is 700 mm. g=9.8 m/s^2 is the gravity acceleration. The opening coefficients of the guide vane a_0, a_1, and a_2 can be calculated by the following.

$$\begin{aligned} a_0 &= 2912x^2 + 5775.4x + 1447.5 \\ a_1 &= 14667x^3 - 31701.8x^2 + 1391.6x - 2873.7 \\ a_2 &= 101707.9x^4 - 248059.7x^3 + 211527.3x^2 \\ &\quad - 59956.7x + 5107 \end{aligned} \tag{15}$$

3. Variable-Universe Fuzzy Control of the Drive Chain for FSR Wind Turbine

Considering that the MPGA algorithm is more stable and faster for continuous function optimization compared with

the standard genetic algorithm (SGA) or particle swarm optimization (PSO) algorithm, which is consequently introduced to optimize the parameters of the extension factor of the variable-universe fuzzy controller (VUFC), in the iteration of SGA, real coding, multipopulation, and multiobjective parallel searching are used for chromosomes, and the minimum preserving algebra of the optimal individual is used as the termination judgment of the algorithm.

In this paper, the designed optimal VUFC was applied to the drive chain for the purpose of speed regulation and torque control of the FSR wind turbine. The objective function is formulated according to the performance of the speed loop. Adaptive control of drive chain is hence realized by adjusting the basic universe adaptively, which thus helps to improve its dynamic and steady performance.

3.1. The Variable Domain Extension Factor. In the design of VUFC, the speed control of drive chain can improve its accuracy according to the variation of expansion factor. The expansion factor, in this sense, can be defined as adjusting the domain of each language control variable according to the value of the current control index.

According to the analysis of two commonly used structures of the expansion factor in [24–26], which points out that the type of proportional-exponential expansion factor satisfies all conditions of the normal expansion factor, a new expansion factor is constructed as provided by

$$\begin{aligned} \alpha(x) &= \omega_1 \left[\frac{|x|}{E}\right]^{\tau_1} \\ \beta(x,y) &= \frac{\omega_2}{2}\left\{\left[\frac{|x|}{E}\right] + \left[\frac{|y|}{EC}\right]\right\}^{\tau_2} \\ \gamma(z) &= \omega_3 \left[\frac{|z|}{U}\right]^{\tau_3} \end{aligned} \tag{16}$$

where $\omega_1 \sim \omega_3$ and $\tau_1 \sim \tau_3$ are six parameters that need to be optimized.

3.2. Design of a Variable-Universe Fuzzy Controller Based on Optimized MPGA. The SGA is a highly parallel, stochastic, and adaptive global optimization probabilistic search algorithm developed from natural selection and evolutionary mechanism of biology, which has strong robustness and global search ability as it does not depend on the gradient. However, with the wide application of SGA, its problem of premature convergence is gradually exposed. It is mainly manifested in the fact that all individuals of the population tend to the same state and stop evolving. As a result, the algorithm cannot give a satisfactory solution. Based on that, this paper proposes to use MPGA to optimize the expansion factor. The schematic of the MPGA algorithm is shown in Figure 3.

In Figure 3, evolutionary mechanism of population 1 to population N is conducted according to SGA. The value of N, in this paper, is determined by tests, which equals 10. The crossing probability and mutation probability are randomly generated in the interval of [0.7, 0.9] and [0.001, 0.05], respectively.

The VUFCs accomplish the expansion of their basic domains by corresponding expansion factors. The expansion of basic domains is equivalent to the adjustment of the control rules. The adaptive law is reflected in the expansion factors α and β. The schematic diagram of the variable universe is shown in Figure 4.

The idea of using MPGA to optimize the VUFC is to let the population, based on selected performance indicators, find the optimal parameters of each expansion factor in each sampling period intelligently relying on the mechanism of global search and local search. After several iterations, the optimal solution of the problem satisfying the performance indicators is thus obtained, which is then taken as the parameter of the expansion factor of the VUFC at the next sampling time. Based on variable-universe theory, an MPGA based variable-universe dual input and single output fuzzy control system for drive chain control of the FSR wind turbine is designed, which is shown in Figure 5.

In Figure 5, $\alpha(x(k))$ and $\beta(x(k), y(k))$ are expansion factors of input variables, respectively. $\gamma(z(k)$ is the expansion factor of the output variable. $x(k)$ and $y(k)$ stand for two input variables of the controller, while $F(x(k), y(k), k)$ represents the control function approximated by the fuzzy controller.

Based on the structure given in Figure 5, the six parameters of the expansion factor are expressed as chromosomes or individuals in the genetic space; the MPGA is used to optimize these parameters and real encoding is hence conducted. The length of the chromosome, in this study, is equal to 6. After acquiring the initial population, six parameters of the expansion factor described in (16) can be assigned to designed fuzzy control system to let the VUFC take over the control. To ensure that the drive chain has a good dynamic performance and the output control variable is within limits, the following objective function is adopted considering the performance of the speed loop of the drive chain:

$$J = \int \left(k_1 |e(t)| + k_2 u^2(t)\right) \mathrm{d}t + k_3 t_{\mathrm{u}} \tag{17}$$

where $u(t)$ is controlled variable, t_{u} is rising time, and k_1, k_2, and k_3 are weights of the objective function.

The adaptive function of individual adaptive value is compiled and calculated according to the objective function, which is given as follows.

$$f = J^{-1} \tag{18}$$

From (18), the adaptive value of each individual can be calculated, which is then provided to the genetic operators for implementing selection, crossover, and mutation to obtain new groups. After iterating for set numbers, the algorithm converges to the best chromosomes and the obtained parameters thus become optimal. Finally, such parameters are assigned to the VUFC for speed regulation of the drive chain. The flow chart of using MPGA to optimize the expansion factor algorithm is shown in Figure 6.

To realize the proposed VUFC optimized by MPGA, the dynamic model of the drive chain, together with the aerodynamics model of the wind turbine and the speed

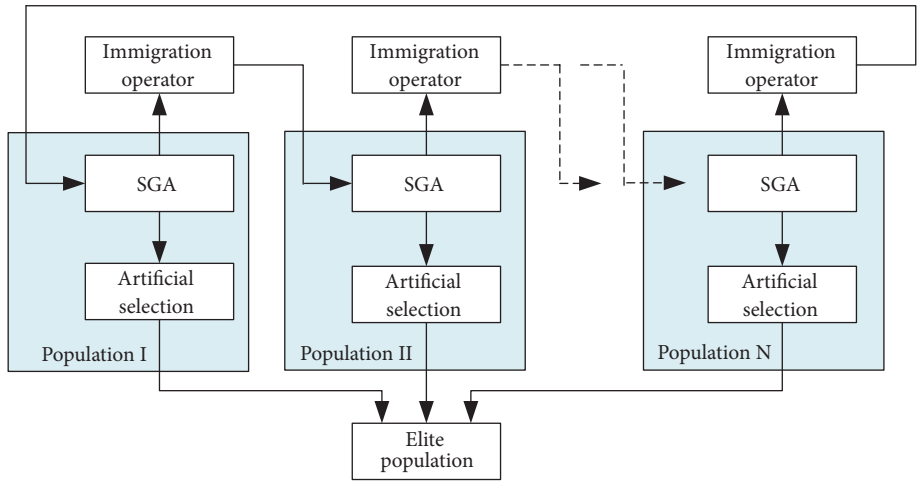

Figure 3: Schematic diagram of the MPGA algorithm.

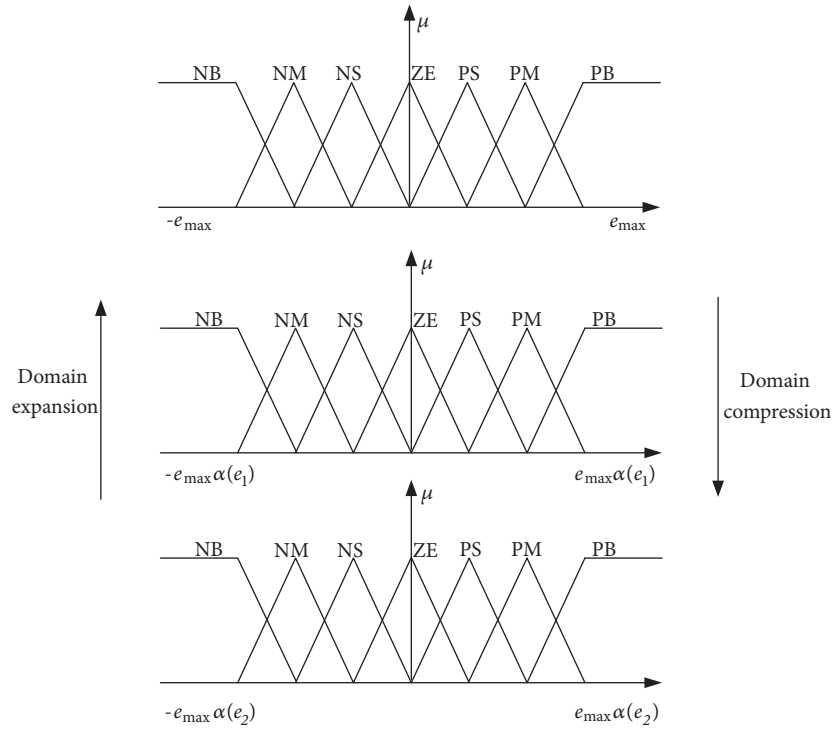

Figure 4: Schematic diagram of the variable universe.

relationship between wind wheel and planetary gears, is implemented in MATLAB/Simulink. Parameters of the wind turbine and drive chain are given in Table 1.

4. Results and Analysis

When implementing the proposed VUFC for drive chain in MATLAB/Simulink using the parameters provided in Table 1, simulation results of the drive chain are thus obtained, which are shown in Figure 7.

As shown in Figure 7(a), the efficiency of hydraulic torque converter first increases and then decreases with the increase of speed ratio. Although the guide vane angle has a certain influence on the efficiency, a peak value indicating the best match between the efficiency and the speed ratio can always be found in the curves.

As shown in Figure 7(b), the turbine speed of the hydraulic torque converter increases with the increase of relative opening angle of the guide vane. When the relative opening angle is 0.5, the turbine speed is about 240 rpm, which will increase to 450 rpm when the relative opening angle is close to 0.9. From either Figure 7(b) or Figure 7(c), it is obvious that the turbine speed can reach a steady value within 0.5 seconds whatever that relative opening angle is. As

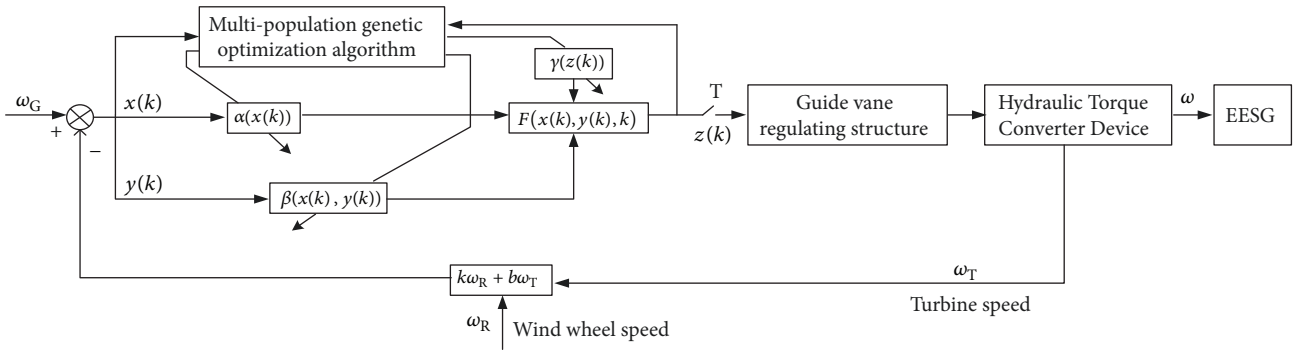

Figure 5: Diagram of variable-universe adaptive fuzzy control system based on MPGA.

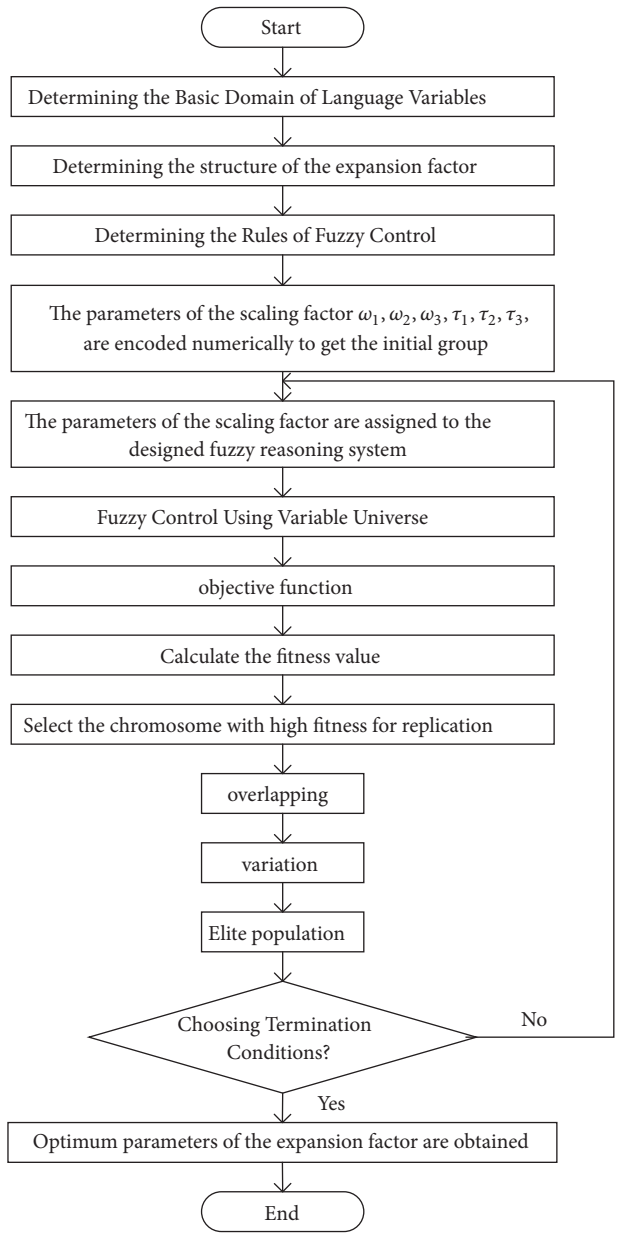

Figure 6: Schematic diagram of the MPGA algorithm.

Table 1: Parameters of the wind turbine and its drive chain used for simulation.

R (m)	ρ (kg/m^3)	β (deg)	J_n (kg·m^2)	J_{t1} (kg·m^2)	J_{t2} (kg·m^2)	J_e (kg·m^2)	T_e (N·m)	c_1	c_e
45.3	1.29	3	875000	10	10	80	300	1380	3.75
Tooth number of the gear ring			Tooth number of solar wheel			Speed Ratio of WinDrive			
161/160			42/74			468/1500			

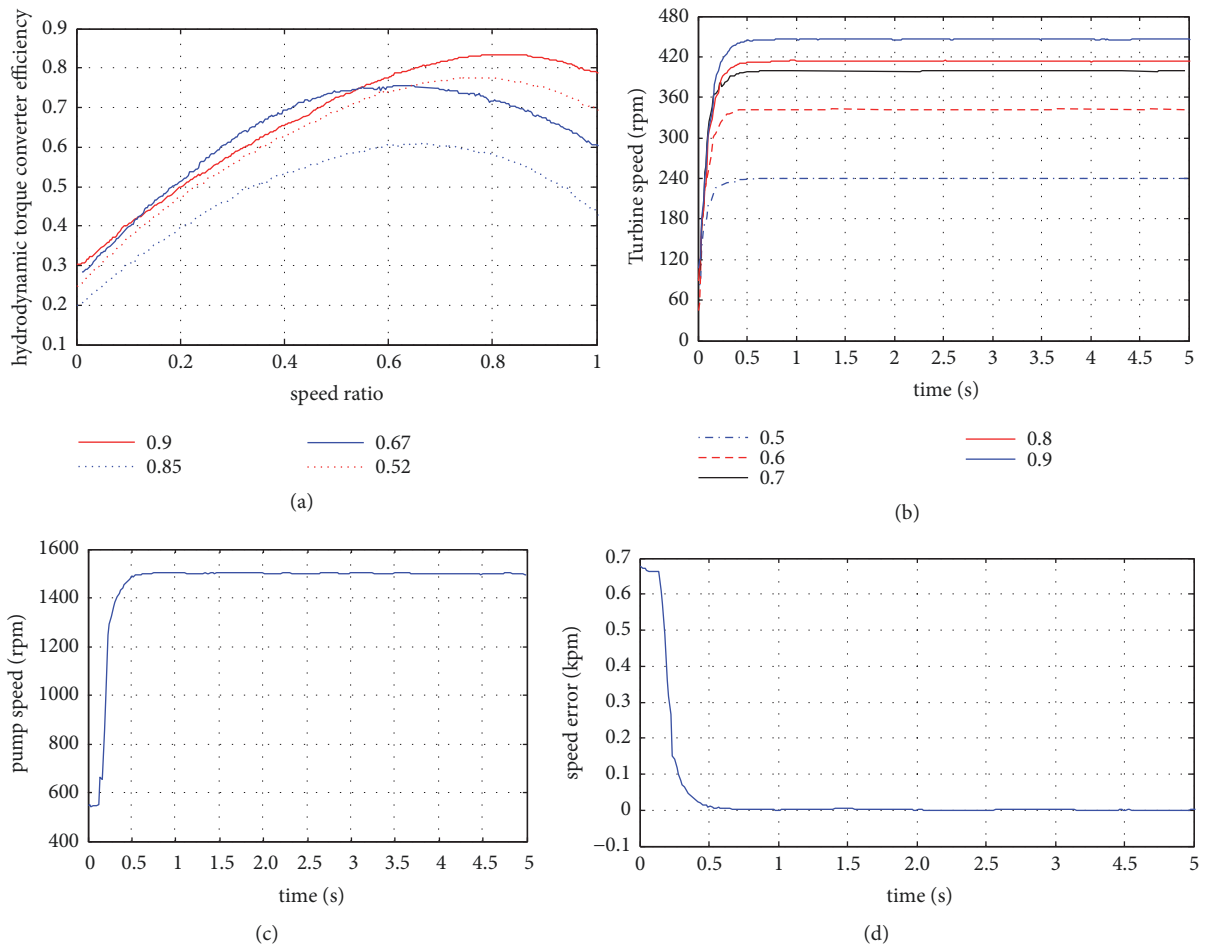

Figure 7: Performance of the proposed VUFC.

shown in Figure 7(c), the pump speed (or the output speed of the hydraulic converter) can reach a steady-state value around 1500rpm. The speed error, as shown in Figure 7(d), after the main shaft speed reaches a steady state, is less than 0.1 rpm. The pump speed and speed error are within a reasonable range, which achieves the purpose of the drive chain design with such a good performance.

For the purpose of comparison, the simulation results using neural network control in [23] are also redrawn in Figure 8.

As shown in Figure 8, once the wind turbine is switched on, the main shaft speed can have a very quick response, and the speed of its main shaft can reach a maximal value, approximately 1630 rpm, in 5 seconds for the neural network controller. An overshoot of 8.7% is produced. After 3 seconds, the main shaft speed of the FSR wind turbine can reach a steady-state value around 1500 rpm. In comparison, the response time of the results derived using VUFC is only less than 0.5 second and there is no overshoot. When focusing on the steady-state performance of two controllers, we obviously see that, from the magnification of Figure 8, the speed error of the neural network controller is much bigger than that of the VUFC.

By comparing the VUFC and the neural network controller, it is clear that the VUFC is more feasible. With the VUFC introduced, the guide vane angle of the hydraulic torque converter can be well adjusted and the output torque of hydraulic torque converter is changed accordingly. The output speed in the control process can adapt to the uncertainty of the input speed, when the VUFC is adopted.

Based on the above analysis, it can be concluded that the simulation model can have a better response to the variation of wind speed, and the wind energy can be captured to the greatest extent when the FSR wind generator operates in a

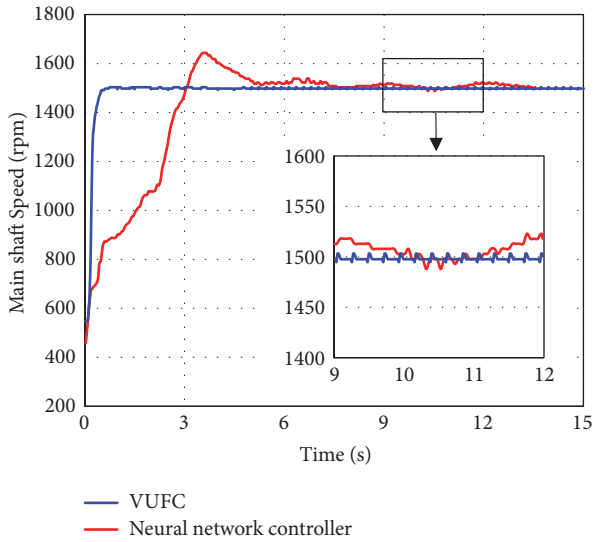

Figure 8: Drive chain performance comparison between the proposed VUFC and the neural network controller.

steady state. The speed of the main shaft or the output speed of the WinDrive can be stabilized near 1500 rpm within only 0.5 seconds, which verifies the outperformance of the VUFC.

5. Conclusions

In this study, the optimized control of drive chain of the FSR wind turbine is realized through a variable-universe fuzzy controller by modeling speed relationship between the wind wheel and the planetary gears, the aerodynamics of the wind turbine, and the dynamics of the drive chain. Compared with the traditional neural network control algorithm, the drive chain control based on multipopulation genetic algorithm improves the control accuracy and speed to a certain extent and ensures reliable operation and quick response of the FSR wind turbine. For the VUFC, a response time less than 0.5 seconds can be achieved to ensure that the main shaft can rotate around 1500 rpm, which is much shorter than a 3-second response utilized with a neural network controller.

Nomenclature

V_w: Wind speed
a: Structure parameter of the first planetary gear set
b,c: Structural parameters of the second planetary gear set
ω_k: Turbine speed
ω_G: Constant speed
x: Guide vane angle
ω_t: Solar wheel speed
ω_j: Speed of planetary gear frame
ω_q: Speed of outer gear ring
ω_T: Output speed of torque converter
ω_R: Wind wheel speed
R: Radius of wind wheel
P_R: Mechanical power
β: Blade angle of the wind wheel
C_P: Power coefficient
λ: Tip speed ratio
ρ: Air density
J_R: Inertial of the wheel
c_1: Coefficient of the low-speed shaft
α: Gear ratio
c_e: Damping coefficient of the high-speed shaft
i: First or second gear set
$J_1 \sim J_4, f_1 \sim f_2$: Coefficient
T_B: Pump torque
T_T: Turbine torque
i_{TB}: Torque converter speed ratio
ρ_{oil}: Density of oil filled in torque converter
λ_B: Torque coefficient of the torque converter pump
n_B: Speed of the torque converter pump
D: Diameter of the circular circle
g: Gravity acceleration
a_0, a_1, a_2: Opening coefficients of the guide vane
$\omega_1 \sim \omega_3, \tau_1 \sim \tau_3$: Optimization parameters
$U(t)$: Control variable
t_u: Rising time
K_1, k_2, k_3: Weights of the objective function.

Data Availability

The data used to support the findings of this study are available from the corresponding author upon request.

Conflicts of Interest

The authors declare that they have no conflicts of interest.

Acknowledgments

This work is financially supported by Scientific Research Projects of Colleges and Universities in Gansu Province (2016b-032).

References

[1] H. Lund, "Renewable energy strategies for sustainable development," *Energy*, vol. 32, no. 6, pp. 912–919, 2007.

[2] M. A. Ortega-Vazquez and D. S. Kirschen, "Estimating the spinning reserve requirements in systems with significant wind power generation penetration," *IEEE Transactions on Power Systems*, vol. 24, no. 1, pp. 114–124, 2009.

[3] G. Raina and O. P. Malik, "Wind energy conversion using a self-excited induction generator," *IEEE Transactions on Power Apparatus and Systems*, vol. 102, no. 12, pp. 3933–3936, 1983.

[4] R. Pena, J. Clare, and G. Asher, "Doubly fed induction generator using back-to-back PWM converters and its application to variable-speed wind-energy generation," in *Proceedings of the Electric Power Applications*, vol. 143, pp. 231–241, no. 3, 2002.

[5] R. Scott Semken, M. Polikarpova, P. Röyttä et al., "Direct-drive permanent magnet generators for high-power wind turbines: Benefits and limiting factors," *IET Renewable Power Generation*, vol. 6, no. 1, pp. 1–8, 2012.

[6] Y. Tang, P. Ju, H. He, C. Qin, and F. Wu, "Optimized control of DFIG-based wind generation using sensitivity analysis and particle swarm optimization," *IEEE Transactions on Smart Grid*, vol. 4, no. 1, pp. 509–520, 2013.

[7] W. La Cava, K. Danai, L. Spector, P. Fleming, A. Wright, and M. Lackner, "Automatic identification of wind turbine models using evolutionary multiobjective optimization," *Journal of Renewable Energy*, vol. 87, pp. 892–902, 2016.

[8] S. M. Mohseni-Bonab, A. Rabiee, and B. Mohammadi-Ivatloo, "Voltage stability constrained multi-objective optimal reactive power dispatch under load and wind power uncertainties: A stochastic approach," *Journal of Renewable Energy*, vol. 85, pp. 598–609, 2016.

[9] B. Yang, L. Jiang, L. Wang, W. Yao, and Q. H. Wu, "Nonlinear maximum power point tracking control and modal analysis of DFIG based wind turbine," *International Journal of Electrical Power & Energy Systems*, vol. 74, pp. 429–436, 2016.

[10] M. Neshati, T. Jersch, and J. Wenske, "Model based active damping of drive train torsional oscillations for a full-scale wind turbine nacelle test rig," in *Proceedings of the 2016 American Control Conference, ACC 2016*, pp. 2283–2288, IEEE, July 2016.

[11] D.-Y. Li, W.-C. Cai, P. Li, Z.-J. Jia, H.-J. Chen, and Y.-D. Song, "Neuroadaptive Variable Speed Control of Wind Turbine with Wind Speed Estimation," *IEEE Transactions on Industrial Electronics*, vol. 63, no. 12, pp. 7754–7764, 2016.

[12] R. Gao and Z. Gao, "Pitch Control for Wind Turbine Systems Using Optimization, Estimation and Compensation," *Journal of Renewable Energy*, vol. 91, pp. 501–515, 2016.

[13] S. Arinaga, T. Wakasa, and T. Matsushita, Coordinated control of power converter and pitch angle for wind turbine generation system, U.S. Patent, vol. 8,242,619, 2012-8-14.

[14] J. Birk and B. Andresen, "Parallel-connected converters for optimizing efficiency, reliability and grid harmonics in a wind turbine," in *Proceedings of the 2007 European Conference on Power Electronics and Applications, EPE*, pp. 1–7, IEEE, Denmark, September 2007.

[15] P. Tenca, A. A. Rockhill, T. A. Lipo, and P. Tricoli, "Current source topology for wind turbines with decreased mains current harmonics, further reducible via functional minimization," *IEEE Transactions on Power Electronics*, vol. 23, no. 3, pp. 1143–1155, 2008.

[16] M. Kesraoui, A. Chaib, A. Meziane, and A. Boulezaz, "Using a DFIG based wind turbine for grid current harmonics filtering," *Energy Conversion and Management*, vol. 78, pp. 968–975, 2014.

[17] A. Hoseinpour, S. Barakati, and R. Ghazi, "Harmonic reduction in wind turbine generators using a Shunt Active Filter based on the proposed modulation technique," *International Journal of Electrical Power & Energy Systems*, vol. 43, no. 1, pp. 1401–1412, 2012.

[18] Y. Rui, J. Chai, and X. Sun, "Variable speed wind turbine based on electromagnetic coupler and its experimental measurement," in *Proceedings of the IEEE PES General Meeting — Conference Exposition*, 2014.

[19] A. Chao, K. Xiangdong, and C. Wenting, "Research on speed control of the main translation system of hydraulic wind energy conversion system," *Acta Energiae Solaris Sinica*, vol. 35, no. 9, pp. 1757–1763, 2014.

[20] P. Lu and W. William, "Principle, structure and application of advanced hydrodynamic converted variable speed planetary gear (Vorecon and Windrive) for industrial drive and wind power transmission," in *Proceedings of the 2011 International Conference on Fluid Power and Mechatronics, FPM 2011*, pp. 839–843, China, 2011.

[21] Z. wei, "Maximum wind energy tracking wind turbine system and simulation," *Electric Machines & Control Application*, vol. 34, no. 5, pp. 42–46, 2007.

[22] R. Li, X. Liu, and S. Liu, "Modelling and simulation of front-end speed adjusting wind turbine drive chain," *Chinese Journal of Mechanical Engineering*, vol. 26, no. 4, pp. 479–484, 2015.

[23] W. Du, *Research on Variable Guide Vane Hydraulic Machinery Speed Regulating Device for Wind Power Generation Investigation*, Jilin University, 2011.

[24] H. Li, "The nature of fuzzy and the design of a class of high precision fuzzy controllers," *Control Theory and Applications*, vol. 14, no. 6, pp. 868–872, 1997 (Chinese).

[25] C. Juang, J. Lin, and C. Lin, "Genetic reinforcement learning through symbiotic evolution for fuzzy controller design," *IEEE Transactions on Systems Man Cybernetics Part B Cybernetics A Publication of the IEEE Systems Man Cybernetics Society*, vol. 30, no. 2, p. 290, 2000.

[26] R. Coban, "A fuzzy controller design for nuclear research reactors using the particle swarm optimization algorithm," *Nuclear Engineering and Design*, vol. 241, no. 5, pp. 1899–1908, 2011.